Chapter 14. Waveguides. (28 Mar 2022)

A. Introduction.

Propagation in waveguides is another form of superposition, one where the waves are confined laterally. In Ch. 12 we superposed waves sharing a common wave vector and called it polarization. In Ch. 13 we coherently superposed waves of different wavelengths but propagating in the same direction and called it short-pulse optics. In Ch. 13 we also superposed waves incoherently, averaged them over time, and found that we could superpose individual intensities.

In Ch. 14 we return to coherently superposing waves of the same frequency but now traveling in different directions. We will find that these superpositions, termed modes, enables us to satisfy boundary conditions that are impossible to satisfy with the plane waves by themselves. The restriction is that all waves share a common phase factor $e^{ik_z z - i\omega t}$, with the result that as the waves move down the guide, net energy transfer occurs in the z direction.

Guides essentially come in three varieties: classic microwave guides, optical fibers, and coaxial cables. The classic guides are hollow metal tubes of usually either rectangular or circular cross section, with confinement being described as the result of the waves reflecting from the walls of the guide. Here, the boundary is an equipotential, which places constraints on the modes that are allowed. Optical fibers are dielectric guides consisting of an inner core and outer sheath, with the refractive index of the core typically higher than that of the sheath. Confinement here can be considered the result of refraction at the core/sheath boundary. However, there is considerable current interest in hollow-core fibers, where confinement is more accurately described as internal reflection. Coaxial cables are another configuration. These consist of inner and outer conductors separated by a dielectric. The existence of two distinct conducting surfaces relaxes the equipotential constraint, with a correspondingly wider range of allowed modes. Paraxial rays, familiar from laser pointers, are another form of lateral localization, but the physics here is diffraction, which is covered in Ch. 16.

The purpose of Ch. 14 is to examine the description and properties of these superpositions. We find that they come in two varieties, transverse magnetic or transverse electric depending on whether the electric or magnetic field, respectively, has a component in the z direction. In

contrast to Ch. 13, "transverse" here refers to the propagation direction, since there is no single plane of incidence. One objective is to develop methods of completely describing these modes in terms of their *z* components. This will turn out to be a particularly convenient way to describe the modes and their properties. In so doing we draw on our skills in solving the two-dimensional Laplace equation, developed in Chs. 5 and 6, with the *z* component assuming the role of the scalar potential. New aspects include energy transfer between sources and these waveguide modes. This is covered in the last section, thereby anticipating the discussion of radiation in Ch. 15.

Throughout the chapter, guides are assumed to be cylindrical, meaning that the cross section of a guide is not necessarily circular, but independent of *z*. Except for optical fibers, covered in Sec. G, we assume that sidewalls are ideal conductors and the medium inside microwave guides is air. With $\varepsilon = \mu = 1$, the individual waves of a mode satisfy $\nabla \cdot \vec{E} = 0$, a condition that will be used to derive the general solution.

In developing the theory of waveguides the same basic strategy applies: start with the fundamental equations, get the math right, and extract the physics from the math. Waveguides provide several excellent examples of the value of this approach.

B. Parallel-plate configuration: general characteristics of waveguide solutions.

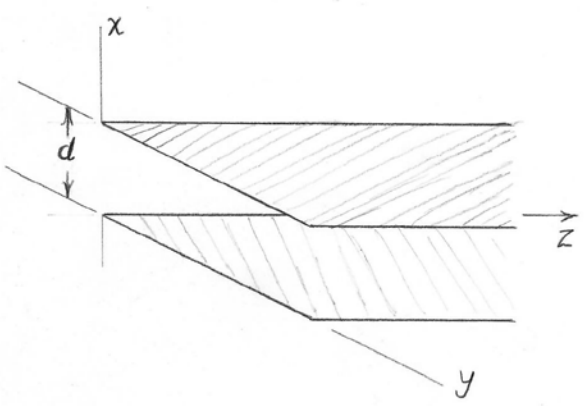

As a tutorial example, consider a one-dimensional guide consisting of two perfectly conducting parallel metal plates separated by a distance *d*, as shown in the figure. The lateral dimensions of the plates are assumed to be much larger than *d*, so edge effects can be ignored. The medium between the plates is air, and propagation occurs in the *z* direction. This is a good entry point to waveguide physics because this transverse-electric (TE) solution is simple enough to be obtained by inspection. It also illustrates how superposition works to satisfy boundary conditions, and the general characteristics of superpositions of plane waves traveling in different directions but sharing a common longitudinal phase factor $e^{ik_z z - i\omega t}$. These solutions exhibit similarities to the coherent superpositions discussed in Ch. 12, having for example phase and group velocities, but new concepts such as cutoff frequency arise. The example differs from treatments below in one aspect: we begin with the transverse electric field instead of determining the *z* component (of the magnetic field) first.

For this configuration the TE solutions are linear combinations of $\vec{E}(\vec{r},t) = \hat{y}E(x)e^{ik_z z - i\omega t}$ that satisfy the boundary conditions and the wave equation. Since tangential components of $\vec{E}$ at an interface with a perfect conductor must be zero, the key relation is $\vec{E}(0,z,t) = \vec{E}(d,z,t) = 0$. Also, for $\mu = \varepsilon = 1$,

$$\left(\nabla^2 - \frac{1}{c^2}\frac{\partial^2}{\partial t^2}\right)\vec{E}(\vec{r},t) = \left(\frac{\partial^2}{\partial x^2} - k_z^2 + \frac{\omega^2}{c^2}\right)\hat{y}E(x)e^{ik_z z - i\omega t}$$

$$= 0\,. \tag{14.1}$$

While the single plane wave $\vec{E}(\vec{r},t) = \hat{y}E_o e^{ik_z z - i\omega t}$ satisfies Eq. (14.1) if $c^2k_z^2 = c^2k^2 = \omega^2$, it can be ruled out because the boundary conditions require $E_o = 0$.

However, a solution consistent with Eq. (14.1) and the boundary conditions can be obtained by forming the linear combination

$$\vec{E}(\vec{r},t) = \frac{1}{2i}\hat{y}\left(e^{ik_x x} - e^{-ik_x x}\right)e^{ik_z z - i\omega t} = \hat{y}E_o \sin(k_x x)e^{ik_z z - i\omega t}\,. \tag{14.2}$$

This is automatically zero at $x = 0$, and also at $x = d$ if $k_x = k_{x\nu} = \frac{\pi\nu}{d}$, where ν is an integer. Thus linear superpositions that satisfy the boundary conditions and Eq. (14.1) exist, but are quantized. In this case the solution consists of a coherent superposition of two plane waves traveling in the directions $\vec{k}_\pm = \pm\hat{x}k_{x\nu} + \hat{z}k_z$.

Substituting Eq. (14.2) into Eq. (14.1) yields the dispersion equation

$$-\left(\frac{\pi\nu}{d}\right)^2 - k_z^2 + \frac{\omega^2}{c^2} = -k_{x\nu}^2 - k_{z\nu}^2 + \frac{\omega^2}{c^2} = 0\,. \tag{14.3}$$

We can write this as

$$c^2k_{z\nu}^2 = \omega^2 - \frac{c^2\pi^2}{d^2}\nu^2 = \omega^2 - \omega_{c\nu}^2\,, \tag{14.4}$$

where $\omega_{c\nu} = c\pi\nu/d$ is the *cutoff frequency*. We note that for $\omega < \omega_{c\nu}$, $k_{z\nu}$ is pure imaginary. In this case the wave does not propagate, but decays exponentially in *z*. It follows by inspection that $\nabla\cdot\vec{E}(\vec{r},t) = 0$.

We see that lateral confinement is possible, but that it comes at a cost: propagation occurs only for frequencies $\omega > \omega_{c\nu}$. As cutoff is approached from above, Eqs. (14.2) and (14.4) show that the constituent waves propagate increasingly in the direction normal to the plates. This also follows from the phase and group velocities $v_{p\nu} = \omega/k_{z\nu}$ and $v_{g\nu} = d\omega/dk_{z\nu}$ that characterize wave packets formed from these solutions, analogous to that which was done in Ch. 12 for plane waves. These velocities are evaluated most easily by working with Eq. (14.4) written as

$$ck_{z\nu} = \sqrt{\omega^2 - \omega_c^2}\,. \tag{14.5}$$

Then

$$v_{p\nu} = \frac{\omega}{k_{z\nu}} = c\frac{\omega}{\sqrt{\omega^2 - \omega_{c\nu}^2}}\,. \tag{14.6}$$

Thus v_{pv} is always greater than *c*, and becomes infinite as $\omega \to \omega_c$ from above. This is consistent with the constituent waves traveling at the speed *c* and reflecting from sidewalls at increasingly normal angles relative to the axis of the guide.

The group velocity is obtained by differentiating Eq. (14.5) by k_{zv} and rearranging coefficients. The result is

$$v_{gv} = \frac{d\omega}{dk_z} = \frac{c^2}{\omega} k_z = c\sqrt{1 - \omega_{cv}^2 / \omega^2} \ . \tag{14.7}$$

Thus v_{gv} is always less than *c*, and vanishes as $\omega \to \omega_{cv}$. This is also consistent with constituent waves propagating increasingly orthogonal to the axis of the guide. As with short-pulse propagation, the concept of a group velocity makes no sense except in connection with wave packets. We note that the same short-pulse procedures used in Ch. 12 can be applied here as well.

The magnetic field and Poynting vector provide additional information. $\vec{H}$ follows from the Faraday-Maxwell Equation. However, because the solution is a superposition of two waves traveling in different directions, the earlier strategy of replacing $\nabla \to i\vec{k}$ is of no help here unless we apply it to the constituents individually. It is now more efficient to evaluate the curl explicitly. The result is

$$\begin{aligned} \vec{H} &= -\frac{ic}{\omega} \nabla \times \vec{E} \\ &= -\frac{cE_o}{\omega} \left(\hat{x}\, k_{zv} \sin k_{xv} x + i\, \hat{z}\, k_{xv} \cos k_{xv} x \right) e^{ik_z z - i\omega t} \ . \end{aligned} \tag{14.8}$$

Equation (14.5) shows that $\vec{H}$ has components in both the *x* and *z* directions, in contrast to $\vec{E}$. Thus the nomenclature TE for this solution.

The transverse nature of $\vec{E}(\vec{r},t)$ suggests that it can be described by taking the cross product of $\vec{H}$ with $\hat{z}$. To assess this, evaluate

$$\hat{z} \times \vec{H} = -\frac{ck_{zv}}{\omega} \hat{y} E_0 \sin(k_{xv} x) e^{ik_{zv} z - i\omega t} \ . \tag{14.9}$$

Thus

$$\vec{E} = \frac{k}{k_{zv}} \hat{z} \times \vec{H} \ , \tag{14.10}$$

where as usual $ck = \omega$. We capitalize below on the fact that the transverse components of $\vec{H}$, and therefore the field $\vec{E}$, can be written in terms of the longitudinal component H_z of $\vec{H}$ alone. This represents a significant simplification, because *z* components are entirely tangential, and hence have simpler boundary conditions. In the next section, we also show that Eq. (14.8) is consistent with the boundary conditions on $\vec{H}$, as expected.

Combining the real projections of Eqs. (14.2) and (14.8), the instantaneous Poynting vector in the propagating range $\omega > \omega_c$ is

$$\vec{S} = \frac{c}{4\pi}\mathrm{Re}(\vec{E}) \times \mathrm{Re}(\vec{H})$$

$$= \frac{c^2 E_o^2}{16\pi\omega}\left(4\hat{z}k_{zv}\sin^2 k_{xv}x\cos^2(k_{zv}z-\omega t) + \hat{x}k_{xv}\sin(2k_{xv}x)\sin(2(k_{zv}z-\omega t))\right). \qquad (14.11)$$

The lateral term vanishes on time averaging, so no net energy propagation occurs in the lateral direction, as expected. Beyond cutoff, $k_{zv} \to i\,|k_{zv}|$, and Eq. (14.11) becomes

$$\vec{S} = \frac{c^2 E_o^2}{16\pi\omega}\left(2\hat{z}k_{zv}\sin^2 k_{xv}x + \hat{x}k_{xv}\sin(2k_{xv}x)\right)\sin(2\omega t)e^{-|k_{zv}|z}. \qquad (14.12)$$

Thus there is no net energy flow in any direction, again as expected.

C. General solution.

We now consider the general solution of the cylindrical waveguide with perfectly conducting walls. Again, "cylindrical" in the present sense means that the walls are independent of *z*, and not necessarily of circular cross section. The magnetic field of the TE wave and the electric field of the TM wave have components in the propagation direction, as noted in Sec. A. In this section we develop the equations that give the lateral components of the wave in terms of its *z* component, and therefore the lateral components of the complementary field as well. Although the final equations are relatively simple, the paths through are not obvious. Accordingly, we work with Cartesian coordinates, where the functions and operations are more familiar.

The starting point is the wave equation for fields. Considering the TM case specifically, we have

$$\left(\nabla(\nabla\cdot\vec{E}) - \nabla^2\vec{E} + \frac{1}{c^2}\frac{\partial^2\vec{E}}{\partial t^2}\right) = 0, \qquad (14.13)$$

where $\vec{E} = \vec{E}(\vec{r},t) = \left(\hat{x}E_x + \hat{y}E_y + \hat{z}E_z\right)e^{ik_z z - i\omega t}$ is assumed to have a *z* component. Now $\vec{E}$ is a linear superposition of plane waves $\vec{E}_j$, each of which satisfies $\nabla\cdot\vec{E}_j = 0$, a consequence of the interior of the guide filled with a material (usually air) with a dielectric function that is isotropic. Thus the superposition must also satisfy $\nabla\cdot\vec{E} = 0$. With the assigned functional dependence $e^{ik_z z - i\omega t}$ of $\vec{E}(\vec{r},t)$ on *z* and *t*, Eq. (14.13) reduces to

$$\left(-\nabla_t^2 + k_z^2 - \frac{\omega^2}{c^2}\right)\vec{E}(\vec{r},t) = 0, \qquad (14.14)$$

where ∇_t^2 is the transverse part of the Lorentzian, or $\nabla_t^2 = \partial^2/\partial x^2 + \partial^2/\partial y^2$ in the present case. As a vector relation, Eq. (14.14) is satisfied individually by each of the three components of $\vec{E}(\vec{r},t)$.

Now consider the trial solution

$$\vec{E}(\vec{r},t) = (\eta\nabla_t + \hat{z})E_z(\vec{r}_t)e^{ik_z z - i\omega t}, \tag{14.15}$$

where η is a constant to be determined. Because $E_z(\vec{r},t)$ satisfies the wave equation, an interchange of the operator $(\eta\nabla_t + \hat{z})$ with that of the wave equation shows that the trial solution satisfies the wave equation as well. However, the trial solution must also satisfy $\nabla\cdot\vec{E} = 0$, which is equivalent to constructing the result as a superposition of transverse waves. Taking the divergence of Eq. (14.15) gives

$$\nabla\cdot\vec{E}(\vec{r},t) = \left(\nabla_t + \hat{z}\frac{\partial}{\partial z}\right)\cdot\left(\eta\nabla_t + \hat{z}\right)\vec{E}(\vec{r}_t,t)e^{ik_z z - i\omega t} \tag{14.16a}$$

$$= \left(\nabla_t^2 + ik_z\right)E_z(\vec{r}_t)e^{ik_z z - i\omega t} = 0. \tag{14.16b}$$

If this equation is to be satisfied, then $E_z(\vec{r}_t)$ must be an eigenfunction of ∇_t^2. Accordingly, let

$$\nabla_t^2 E_z(\vec{r}_t) = -k_t^2 E_z(\vec{r}_t), \tag{14.17a}$$

where k_t is the lateral component of $\vec{k}$. Thus

$$\eta = ik_z/k_t^2. \tag{14.17b}$$

The task of determining $E_z(\vec{r}_t)$ has just been reduced to a two-dimensional eigenfunction/eigenvalue problem familiar from Chs. 5 and 6, with $E_z(\vec{r}_t)$ taking the place of $\phi(\vec{r},t)$. The complete solution for $\vec{E}(\vec{r},t)$ is therefore

$$\vec{E}(\vec{r},t) = \left(\frac{ik_z}{k_t^2}\nabla_t + \hat{z}\right)E_z(\vec{r}_t)e^{ik_z z - i\omega t}. \tag{14.18}$$

This is a general result, independent of the coordinate system involved.

Given Eq. (14.18), the associated magnetic field can be calculated directly from the Faraday-Maxwell Equation. We can save some work by adding and subtracting $\hat{z}(\partial/\partial z)$ to convert ∇_t into $\nabla = \nabla_t + \hat{z}\partial/\partial z$, then take advantage of the fact that the curl of a gradient is zero. The calculation evolves as

$$\nabla\times\vec{E}(\vec{r},t) = \nabla\times\left(\frac{ik_z}{k_t^2}(\nabla_t + \hat{z}\frac{\partial}{\partial z}) - \frac{ik_z}{k_t^2}\hat{z}\frac{\partial}{\partial z} + \hat{z}\right)E_z e^{ik_z z - i\omega t} \tag{14.19a}$$

$$= \nabla\times\left(\left(\frac{ik_z}{k_t^2}\nabla + \frac{k_z^2}{k_t^2}\hat{z} + \hat{z}\right)E_z(\vec{r}_t)e^{ik_z z - i\omega t}\right) \tag{14.19b}$$

$$= \left(\frac{k_z^2}{k_t^2} + 1\right)\nabla\times\left(\hat{z}E_z(\vec{r}_t)e^{ik_z z - i\omega t}\right). \tag{14.19c}$$

Completing the calculation gives

$$\vec{H}(\vec{r},t) = -\frac{ik}{k_t^2}\left(\hat{x}\frac{\partial E_z}{\partial y} - \hat{y}\frac{\partial E_z}{\partial x}\right)e^{ik_z z - i\omega t}. \tag{14.20}$$

The form of Eq. (14.20) is that of a vector cross product. Accordingly, construct $\hat{z}\times\vec{E}$, where $\vec{E}$ is given in Eq. (14.18). The result is

$$\hat{z}\times\vec{E}(\vec{r},t) = \frac{ik_z}{k_t^2}\left(\hat{y}\frac{\partial E_z}{\partial x} - \hat{x}\frac{\partial E_z}{\partial y}\right)e^{ik_z z - i\omega t}. \tag{14.21}$$

By comparing Eqs. (14.20) and (14.21), we see that

$$\vec{H}(\vec{r},t) = \frac{k}{k_z}\hat{z}\times\vec{E}. \tag{14.22}$$

where as usual $ck = \omega$. This relation is particularly simple, and illustrates the transverse nature of $\vec{H}$ directly for the TM mode.

When k_z is real, Eq. (14.22) shows that the real projections of $\vec{E}$ and $\vec{H}$ are in phase, so energy transport occurs. Beyond cutoff k_z is imaginary, so these real projections are 90° out of phase and the instantaneous Poynting vector time-averages to zero. Thus energy transport beyond cutoff is not possible, as seen for the parallel-plate example in Sec. B.

The calculation for TE modes proceeds similarly. $\vec{H}(\vec{r},t)$ can be replaced with $\vec{E}(\vec{r},t)$ and vice versa, with appropriate boundary-condition and sign changes. The results are

$$\vec{H}(\vec{r},t) = \left(\frac{ik_z}{k_t^2}\nabla_t + \hat{z}\right)H_z(\vec{r}_t)e^{ik_z z - i\omega t}; \tag{14.23a}$$

$$\vec{E}(\vec{r},t)) = \frac{ik}{k_t^2}\left(\hat{x}\frac{\partial H_z}{\partial y} - \hat{y}\frac{\partial H_z}{\partial x}\right)e^{ik_z z - i\omega t}. \tag{14.23b}$$

$$= -\frac{k}{k_z}\hat{z}\times\vec{H}(\vec{r}) \tag{14.23c}$$

We therefore have a complete solution, valid for cylindrical guides of perfectly conducting walls of any cross section.

As an example, consider a guide of rectangular cross section of dimensions *a* and *b* along *x* and *y*, respectively. The solution $E_z(\vec{r}_t)$ that satisfies the dispersion equation and boundary conditions is

$$E_z(\vec{r}_t,z,t) = E_{z\mu\nu}\sin\left(\mu\frac{\pi}{a}\right)\sin\left(\nu\frac{\pi}{b}\right)e^{ik_z z - i\omega t}, \tag{14.24}$$

where μ and ν are integers,

$$k_t^2 = k_{t,\mu\nu}^2 = k_{x,\mu\nu}^2 + k_{y,\mu\nu}^2 = \pi^2\left(\frac{\mu^2}{a^2} + \frac{\nu^2}{b^2}\right), \tag{14.25}$$

and

$$k_z^2 = k_{z,\mu\nu}^2 = \frac{\omega^2}{c^2} - k_{t\mu\nu}^2 = \frac{\omega^2}{c^2} - \pi^2\left(\frac{\mu^2}{a^2} + \frac{\nu^2}{b^2}\right). \tag{14.26}$$

The electric field is

$$\vec{E}_{TM}(\vec{r},t) = E_o\left(\frac{ik_z}{k_t^2}\left(\hat{x}k_x \cos k_x x \sin k_y y + \hat{y}k_y \sin k_x x \cos k_y y\right) + \hat{z}\sin k_x x \sin k_y y\right)e^{ik_z z - i\omega t} \tag{14.27}$$

where $k_x = \mu\pi/a$ and $k_y = \nu\pi/b$. The magnetic field is

$$\vec{H}_{TM}(\vec{r},t) = -\frac{ikE_o}{k_t^2}\left(\hat{x}k_y \sin k_x x \cos k_y y - \hat{y}k_x \cos k_x x \sin k_y y\right)e^{ik_z z - i\omega t}. \tag{14.28}$$

After more algebra, the *z* component of the cycle-averaged Poynting vector for a propagating mode is

$$< \vec{S}_{TM} > = \hat{z}\frac{c}{8\pi}\frac{\omega k_z}{ck_t^4}E_o^2\left(k_x^2 \cos^2 k_x x \sin^2 k_y y + k_y^2 \sin^2 k_x x \cos^2 k_y y\right). \tag{14.29}$$

As a cross-check, the intensity is in the positive *z* direction. The one-dimensional example of Sec. B is Eq. (14.27) in the limit $k_x \to 0$.

The corresponding solutions for the TE modes are

$$H_{z,TE}(\vec{r}_t, z, t) = H_{z\mu\nu}\cos\left(\mu\frac{\pi}{a}\right)\cos\left(\nu\frac{\pi}{b}\right)e^{ik_z z - i\omega t}, \tag{14.30a}$$

$$\vec{H}_{TE}(\vec{r},t) = H_o\left(-\frac{ik_z}{k_t^2}\left(\hat{x}k_x \sin k_x x \cos k_y y + \hat{y}k_y \cos k_x x \sin k_y y\right) + \hat{z}\cos k_x x \cos k_y y\right)e^{ik_z z - i\omega t}, \tag{14.30b}$$

$$\vec{E}_{TE}(\vec{r},t) = \frac{ikH_o}{k_t^2}\left(\hat{x}k_y \cos k_x x \sin k_y y - \hat{y}k_x \sin k_x x \cos k_y y\right)e^{ik_z z - i\omega t}. \tag{14.30c}$$

In the design of microwave systems, the number of modes that can propagate and their cutoff frequencies are part of the usual engineering criteria. From Eq. (14.24), the lowest TM mode is that for which $(\mu,\nu) = (1,1)$. From Eq. (14.30a), the lowest TE mode is either $(0,1)$ or $(1,0)$ depending on whether $b > a$ or whether the inequality is reversed. Hence the TE mode is the lowest overall mode of the configuration. In practice, single-mode operation is desired. This allows receiving and transmitting antennas to be configured for maximum overlap with the cross section of the mode, and therefore maximum efficiency (see Sec. J). This also minimizes scattering from defects, which decreases efficiency as a result of energy being diverted into parasitic modes.

D. Boundary conditions.

Boundary conditions impose restrictions on allowed solutions, as we saw in Sec. B. Because these involve fields, not scalars, these can be confusing. Not all are as simple as these, so a

discussion is warranted. Although there are only two kinds of fields, electric and magnetic, each has three components, and constraints occur not only for components parallel to sidewalls but in more general situations as well. Referring to the diagram, which focuses on the *xz* sidewall of a hypothetical rectilinear guide, the locally parallel components of the electric field are E_x and E_z, and the normal component is E_y. These are fields in the guide cavity, not in the guide walls themselves. In addition to the three component values there are 4 types of derivatives: (1) the tangential derivatives of the tangential components, or $\partial E_x/\partial x$, $\partial E_x/\partial z$, $\partial E_z/\partial x$, and $\partial E_z/\partial z$; (2) the normal derivatives of the same components, or $\partial E_x/\partial y$ and $\partial E_z/\partial y$; (3) the tangential derivative of the normal components, or $\partial E_y/\partial x$ and $\partial E_z/\partial y$; and (4) the normal derivative of the normal component, or $\partial E_y/\partial y$. We use this diagram throughout this section, replacing the components of $\vec{E}$ with those of $\vec{H}$ when needed. Our task is to determine the conditions on these quantities on the sidewalls of the guide.

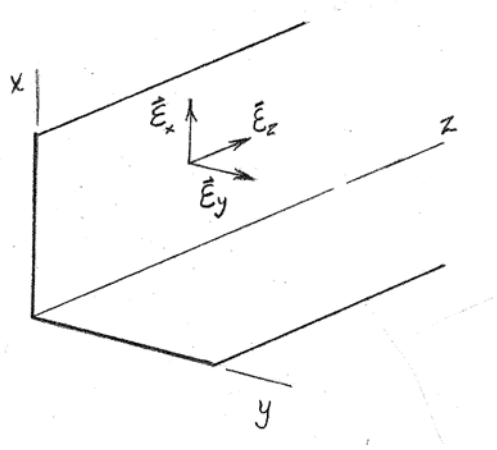

Considering first the electric field, Stokes' Theorem applied to the Faraday-Maxwell Equation shows that the tangential components E_x and E_z are zero at the sidewall of a perfect conductor. Because $E_x = E_z = 0$ everywhere on the sidewall, it follows that the tangential derivatives $\partial E_x/\partial x = \partial E_x/\partial z = \partial E_z/\partial x = \partial E_z/\partial z = 0$ there as well.

Next, consider

$$\nabla \cdot \vec{E} = \frac{\partial E_x}{\partial x} + \frac{\partial E_y}{\partial y} + \frac{\partial E_z}{\partial z} = 0, \tag{14.31}$$

which follows because the cavity contains no charge. But we have just shown that at the sidewall $\partial E_x/\partial x = \partial E_z/\partial z = 0$, since these are tangential derivatives of tangential components. Hence at the sidewall

$$\frac{\partial E_y}{\partial y} = 0 \tag{14.32}$$

as well.

Why does this matter? Consider a rectilinear resonant cavity, which is a waveguide capped at two ends (see diagram.) If there were no constraints on the normal component of the electric field, then any frequency above cutoff would be an allowed solution, However, applying what we have just derived, the only allowed modes are those for which $\partial E_z/\partial z = 0$ at the end caps, or

$$E_z(\vec{r},t) = E_o \sin\left(\frac{\pi l}{a}x\right)\sin\left(\frac{\pi m}{a}y\right)\cos\left(\frac{\pi n}{a}z\right), \tag{14.33}$$

where *l*, *m*, and *n* are integers. Thus ω cannot assume arbitrary values but is restricted to the discrete values

$$\omega = \omega_{lmn} = c\sqrt{\left(\frac{\pi l}{a}\right)^2 + \left(\frac{\pi m}{b}\right)^2 + \left(\frac{\pi n}{d}\right)^2}\ . \tag{14.34}$$

These resonances are obviously the normal modes of the cavity. The fields in the *x* and *y* directions follow as usual. It can be appreciated from Eq. (14.33) that the solution for a given set of quantum numbers consists of standing waves formed as a linear superposition of two plane waves in each direction.

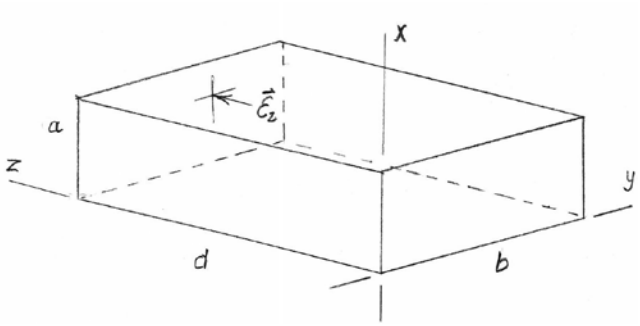

Of the 6 classes of boundary functions, we have now investigated three. The next is the normal field $\vec{E}_y$. Gauss' Theorem applied to Gauss' Law shows that this imposes no constraint because a perfect conductor delivers whatever surface charge density σ is necessary to prevent $\vec{E}_y$ from penetrating into the conductor. Thus σ follows from $\vec{E}_y$, which in turn follows from the solution. Similarly, the tangential derivatives $\partial E_y/\partial x$ and $\partial E_y/\partial z$ of the normal field are not constraints, but also follow from the solution. Finally, there is no constraint on the normal derivatives of the tangential solutions $\partial E_x/\partial y$ and $\partial E_z/\partial y$. These too follow from the solution. For the rectilinear guide it is easily verified that all conditions are also satisfied by the transverse fields $\vec{E}_t = \frac{ik_z}{k_t^2}\nabla_t E_z$.

The magnetic field component H_z can be treated similarly, but the calculations are less direct. Stokes' Theorem and Ampère's Equation applied to a path passing through the conductor and the guide cavity show that the tangential magnetic fields H_x and H_z generate a surface current $\vec{K}$. Analogous to σ in the electric-field case, this is a recipe for determining $\vec{K}$, which follows from H_z and H_x, which in turn follow from the solution. Accordingly, the tangential derivatives of these quantities, for example $\partial H_z/\partial x$ and $\partial H_z/\partial z$, follow from the solution as well.

The simplest magnetic constraint involves the perpendicular component H_y. With $\nabla\cdot\vec{B} = \nabla\cdot\vec{H} = 0$ and Gauss' Theorem, the normal component of $\vec{B} = \vec{H}$ is continuous at the guide-cavity interface. Now consider $\nabla\times\vec{E} + \frac{1}{c}\frac{\partial\vec{B}}{\partial t} = 0$. This equation shows that any time-dependent field $\vec{B}$ in a conductor is accompanied by an electric field. But an electric field cannot exist in a perfect conductor. Hence a magnetic field cannot exist there either. Hence the normal component of $\vec{H}$ at a wall must be zero as well. With $H_y = 0$, it follows that the tangential derivatives $\partial H_y/\partial x$ and $\partial H_y/\partial z$ must also be zero. The normal derivative of the normal component, $\partial H_y/\partial y$, has no local constraint and is determined by the solution.

However, the normal derivatives of the tangential components $\partial H_x/\partial y$ and $\partial H_z/\partial y$ are constrained, which we show next. This is clearly relevant for H_z. The constraint again follows from a constraint on the electric field. Ampère's Equation states explicitly

$$-\frac{i\omega}{c}\vec{E} = \nabla \times \vec{H} = -\begin{pmatrix} \hat{x} & \hat{y} & \hat{z} \\ \frac{\partial}{\partial x} & \frac{\partial}{\partial y} & \frac{\partial}{\partial z} \\ H_x & H_y & H_z \end{pmatrix}. \tag{14.35}$$

Consider E_x, which is tangential to the wall and therefore vanishes. Then

$$-i\frac{\omega}{c}E_x = \frac{\partial H_z}{\partial y} - \frac{\partial H_y}{\partial z} = 0. \tag{14.36}$$

But we have already shown that $\partial H_y/\partial z = 0$ at the wall. Therefore, $\partial H_z/\partial y = 0$ at the wall as well. Similarly $\partial H_x/\partial y = 0$. Thus the normal derivative of the tangential components of $\vec{H}$ must equal zero. The allowed TE modes corresponding to Eq. (14.33) are therefore

$$H_z(\vec{r},t) = H_o \cos\left(\frac{\pi l}{a}x\right)\cos\left(\frac{\pi m}{a}y\right)\sin\left(\frac{\pi n}{a}z\right). \tag{14.37}$$

The remaining derivatives are not conditions, but follow from the solution. The situation is summarized in Table I. Note that, as usual with Maxwell's Equations, $\vec{E}$ and $\vec{H}$ are complementary. Again, it is straightforward to show that the *x* and *y* components of $\vec{H}$ satisfy these conditions as well, as they must.

Table I: Boundary conditions for propagating waves at the surface of a perfect conductor.

$\vec{E}$	Constraint:	$\vec{H}$	Constraint:
Tangential components E_x, E_z:		Tangential components H_x, H_z:	
Values	= 0	Values	(soln. gives $\vec{K}$)
Tangential derivatives	= 0	Tangential derivatives	(from soln.)
Normal derivatives	(from soln.)	Normal derivatives	= 0
Normal component E_y:		Normal component H_y:	
Value	(soln. gives σ)	Value	= 0
Tangential derivatives	(from soln.)	Tangential derivatives	= 0
Normal derivative	= 0	Normal derivative:	(from soln.)

E. Resonant cavities continued.

We have already introduced the *z* components of the TM and TE modes in Eqs. (14.33) and (14.37), respectively. The complete fields are given by applying the equations derived earlier with one exception: because the *z* components now consist of waves propagating in both

directions, it is not possible to use Eq. (14.23c) and its TE equivalent directly. They can be applied individually to the two complex exponentials that make up $\cos k_z z$ and $\sin k_z z$, but not to the harmonic functions themselves. In fact this calculation is unnecessary: the high symmetry of the rectilinear cavity allows the transverse fields to be written by inspection. For the TM case the complete field is

$$\vec{E}_{lmn}^{TM}(\vec{r},t) = -\hat{x}\frac{k_x k_z}{k_t^2}E_{lmn}\cos k_x x \sin k_y y \sin k_z z e^{-i\omega_{lm0}t}$$

$$-\hat{y}\frac{k_y k_z}{k_t^2}E_{lmn}\sin k_x x \cos k_y y \sin k_z z\, e^{-i\omega_{lm0}t}$$

$$+\hat{z}\,E_{lmn}\sin k_x x \sin k_y y \cos k_z z\, e^{-i\omega_{lm0}t}, \qquad (14.38)$$

and

$$\vec{H}_{lmn}^{TM}(\vec{r},t) = \hat{x}\frac{k_y k}{k_t^2}E_{lmn}\sin k_x x \cos k_y y \cos k_z z\, e^{-i\omega_{lmn}t}$$

$$-\hat{y}\frac{k_x k}{k_t^2}E_{lmn}\cos k_x x \sin k_y y \cos k_z z\, e^{-i\omega_{lmn}t}. \qquad (14.39)$$

It can be seen that the boundary conditions listed in Table 1 are satisfied in all cases. Further, it also follows by inspection of the structure of the equations that $\nabla\cdot\vec{E} = \nabla\cdot\vec{H} = 0$, in the former case taking advantage of the relation $k_t^2 = k_x^2 + k_y^2$. With standing waves in all three dimensions, the only remaining variable in the dispersion equation is $\omega = \omega_{lmn}$, which is

$$\left(\frac{\pi l}{a}\right)^2 + \left(\frac{\pi m}{b}\right)^2 + \left(\frac{\pi n}{d}\right)^2 = \frac{\omega_{lmn}^2}{c^2} \qquad (14.40)$$

for both TE and TM modes, where *l*, *m*, and *n* are integers or zero. This last degree of freedom is fixed by the geometry.

A typical objective is to find the lowest mode. Considering first the TM case, it is clear that setting either l or *m* equal to zero eliminates the mode, so this is not permitted. With $n = 0$, $\vec{E}(\vec{r})$ reduces to a constant field in the *z* direction. Whether this represents a viable solution can be answered by assessing $\vec{H}$. In this case Eq. (14.33) reduces to

$$\vec{E}_{lm0}^{TM}(\vec{r}_t,z,t) = \hat{z}\,E_{lm0}\sin\left(\frac{\pi l}{a}x\right)\sin\left(\frac{\pi m}{b}y\right)e^{-i\omega_{lm0}t}. \qquad (14.41)$$

With $k_z = 0$ no *x* and *y* components exist, so $\nabla\cdot\vec{E} = 0$ trivially. The standard calculation yields

$$\vec{H}^{TM}(\vec{r}_t,z,t) = \hat{x}E_{lm0}k_y\sin(k_x x)\cos(k_y y)e^{-i\omega_{lm0}t}$$

$$-\hat{y}E_{lm0}k_x\cos(k_x x)\sin(k_y y)e^{-i\omega_{lm0}t}. \qquad (14.42)$$

These modes are both viable, and $\nabla \cdot H_{lm0}^{TM} = 0$ by inspection. Thus this mode passes all tests, and is the lowest TM mode.

For the TE mode, the complete magnetic and electric fields are

$$\vec{H}_{lmn}^{TE}(\vec{r}_t, z, t) = \hat{x}\, H_{lmn} \sin k_x x \cos k_y y \cos k_z z\, e^{-i\omega_{lmn}t}$$
$$+ \hat{y}\, H_{lmn} \cos k_x x \sin k_y y \cos k_z z\, e^{-i\omega_{lmn}t}$$
$$+ \hat{z}\, H_{lmn} \cos k_x x \cos k_y y \sin k_z z\, e^{-i\omega_{lmn}t}; \qquad (14.43a)$$

$$\vec{E}_{lmn}^{TE} = \frac{ic}{\omega} H_{lmn} \left(\hat{x} k_y \cos k_x x \sin k_y y - \hat{y} k_x \sin k_x x \cos k_x y \right) e^{-i\omega_{lmn}t}. \qquad (14.43b)$$

The symmetry between the solutions $\vec{E}_{lmn}^{TM}$ and $\vec{H}_{lmn}^{TE}$ can be noted. While it is tempting to suppose from $\vec{H}$ that the lowest mode is $(0,0,1)$, it follows from $\vec{E}$ electric field for a hypothetical $(0,0,1)$ mode would not exist. Consequently, the lowest mode is either $(0,1,1)$ or $(1,0,1)$ depending on whether $b > a$ or vice versa. Picking $a > b$ we set $l = 1$ and $m = 0$, and verify that all conditions are met. We leave details to a homework exercise. In the final analysis the answer depends on the ordering of the dimensions *a*, *b*, and *d*.

F. Guides of circular cross section.

Guides with circular cross sections provide a good opportunity to review what we learned in Ch. 6 last semester. Consider first the electrostatic solution corresponding to the TM modes. For the potential specified on the $z = 0$ face with $\phi(\vec{r}) = 0$ at $\rho = a$ and $z = d$, one possible solution of the two-dimensional eigenvalue problem is

$$\left(\frac{1}{\rho} \frac{\partial}{\partial r} \left(\rho \frac{\partial}{\partial \rho} \right) + \frac{1}{\rho^2} \frac{\partial^2}{\partial \varphi^2} + \frac{\partial^2}{\partial z^2} \right) \phi(\rho, \varphi, z)$$
$$= \left(-k_t^2 + k_z^2 \right) J_\nu(x_{\nu n} \rho / a) e^{i\nu\varphi} \sinh\left(k_z (d - z) \right) = 0. \qquad (14.43c)$$

The last equation forces the electrostatic condition $k_z^2 = k_t^2$, where $x_{\nu n}$ is the n^{th} zero of $J_\nu(x)$.

However, with the extra degree of freedom provided by the time operator in the wave equation, the equivalent waveguide expression is

$$\left(\nabla^2 - \frac{1}{c^2} \frac{\partial^2}{\partial t^2} \right) E_z(\rho, \varphi) e^{ik_z z - \omega t} = \left(-k_t^2 - k_z^2 + \frac{\omega^2}{c^2} \right) E_z(\rho, \varphi) e^{ik_z z - i\omega t}. \qquad (14.44)$$

k_z^2 and k_t^2 are now decoupled, and the previous condition $k_t^2 = k_z^2$ is replaced by $k_t^2 = (-k_z^2 + \omega^2 / c^2)$. This allows an oscillatory function (the wave $e^{ik_z z}$) to appear in the *z* direction. The rest is electrostatics.

The situation for the TE case is similar, except that the TE boundary condition is that the normal derivative of the normal component equals zero at the boundary. Thus for $H_z(\rho,\varphi)$ the relevant numbers are the zeroes of the derivatives of the Bessel functions. Jackson gives the values of some of these zeroes in Sec. 8.7. The "lowest-mode' calculation makes the results worth repeating here:

Table II: Zeroes of Bessel functions and their derivatives

$J_\nu(x)$ (TE):				$J_\nu'(x)$ (TM):		
n, ν:	0	1	2	0	1	2
1	2.404	3.382	5.136	0.000	1.841	3.054
2	5.520	7.016	8.417	3.831	5.331	6.706
3	8.653	10.173	11.620	7.016	8.536	9.969

Recalling that

$$k_z^2 = \frac{\omega^2}{c^2} - k_{\nu n}^2 = \frac{\omega^2}{c^2} - \frac{x_{\nu n}^2}{a^2}, \tag{14.45}$$

the mode that can operate with the smallest diameter waveguide, or conversely has the smallest cutoff frequency is the (1,1) TM mode. This follows because the first maximum of $J_1(x)$ occurs at a smaller value of x than the first zero crossing of $J_0(x)$.

G. Optical fibers.

As Jackson notes at the beginning of his Sec. 8.10, "optical fibers lie at the heart of high-speed, high-capacity telecommunications." The rest of Jackson's section is devoted entirely to multimode fibers, where the diameter of the active region is typically of the order of 50 μm, i.e., many times larger than the c-band communications wavelengths of 1.53 to 1.56 μm (wavelengths of 1.07 to 1.10 μm in the fiber). While multimode fibers continue to be used in short-haul (several-m) applications, long-haul (100 km on up) applications use single-mode fiber exclusively. Since their cores are relatively large, multimode fibers have the advantage that it is easy to get radiation into them, so the associated lasers are cheaper and alignment is less critical. However, since different modes have different group velocities, the constituent waves of the short pulses arrive at different times, even if they all start the same. This degradation limits either the distance between sources and receivers, or data rates, as we have seen in Ch. 13.

Multimode fibers are essentially light pipes that operate on the principle of total internal reflection. The first such "light pipe" was demonstrated by Colladon in 1842. This was a "light fountain", where he showed that a beam of light would follow the curvature of a stream of water emerging from a source. The physics is nothing more than total internal reflection, which we have already covered. Details include descriptions of various paths, and estimates of the spreading of a signal by the time it reaches the end of the fiber. Jackson discusses two types: meridional rays that bounce back and forth making multiple passes through the cylinder axis, and skew rays that essentially follow a spiral path through the fiber. He discusses the mathematics of

calculating transit times, but for current application this is not particularly interesting. Consequently, we focus our attention on single-mode fibers.

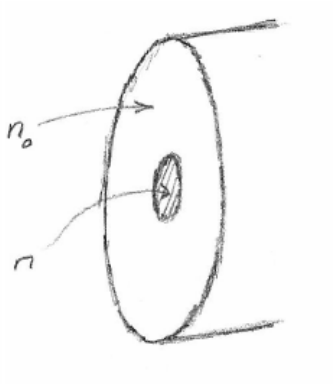

A sketch of the cross section of a single-mode optical fiber is shown at the right. The core, subscript 1, is typically about 8 to 10 μm in diameter and consists of a silica alloy with a refractive index n_1 that is slightly larger than that of the cladding, n_2, for reasons that will become clear below. The cladding, subscript 2, is considerably thicker than the core, again for reasons that will become clear below. The description of single-mode fibers is simplified because, as the name implies, they are designed such that only one mode can propagate in them. All other modes are beyond cutoff. The propagating mode is the so-called (0,0) mode, i.e., the lowest TM mode with radial function $J_0(k_{t1}\rho)$ in the core, for which the spatial dependence is entirely radial. The matching function in the cladding is the exponentially decreasing mode $K_0(k_{t2}\rho)$, with the connection established by the fact that both share the same spatial and temporal dependence $e^{ik_z z - i\omega t}$, a consequence of the usual boundary conditions on tangential $\vec{E}$ and $\vec{H}$. An outline of the math involved follows.

We begin with the wave and dispersion equations. Dispensing with the term $\nabla(\nabla\cdot\vec{E})$, for the core we have

$$\left(-\frac{1}{\rho}\frac{\partial}{\partial\rho}\left(\rho\frac{\partial}{\partial\rho}\right)-\frac{1}{\rho^2}\frac{\partial^2}{\partial\varphi^2}-\frac{\partial^2}{\partial z^2}+\frac{\varepsilon_1}{c^2}\frac{\partial^2}{\partial t^2}\right)\vec{E}_1(\vec{r},t)=0\,. \tag{14.46}$$

Going several steps further, we insert the eigenfunction $e^{i\nu\varphi}$ for φ and the usual *z* and *t* dependences for waveguides, obtaining

$$\left(\frac{1}{\rho}\frac{\partial}{\partial\rho}\left(\rho\frac{\partial}{\partial\rho}\right)-\frac{\nu^2}{\rho^2}-k_z^2+\frac{\omega^2\varepsilon_1}{c^2}\right)\vec{E}_1(\vec{r},t)=0\,. \tag{14.47}$$

Comparing the above to Bessel's Equation,

$$\left(\frac{1}{\rho}\frac{\partial}{\partial\rho}\left(\rho\frac{\partial}{\partial\rho}\right)-\frac{\nu^2}{\rho^2}-k_{t1}^2\right)J_\nu(k_{t1}\rho)=0\,, \tag{14.48}$$

we see that terms can be eliminated if $E_{z1}(\rho)=E_{o1}J_\nu(k_{t1}\rho)$ and k_{t1}^2 is appropriately added and subtracted. The result is

$$\left(-k_{t1}^2-k_z^2+\frac{\omega^2\varepsilon_1}{c^2}\right)J_\nu(k_{t1}\rho)e^{i\nu\varphi}e^{ik_z z-i\omega t}=0\,, \tag{14.49a}$$

where

$$E_{z1}(\rho,\varphi,z,t)=E_{o1}J_\nu(k_{t1}\rho)e^{i\nu\varphi}e^{ik_z z-i\omega t}\,. \tag{14.49b}$$

Thus one of the equations that must be satisfied is the dispersion equation of the core:

$$k_{t1}^2 + k_z^2 = \frac{\omega^2 \varepsilon_1}{c^2}, \tag{14.50}$$

where k_{t1} and k_z are real. Ordinarily we would obtain k_{t1} by applying boundary conditions at the core diameter $\rho = a$, but the field now penetrates into the cladding. Since the Laplacian no longer equals zero, k_z no longer equals k_{t1}, as it did in electrostatics.

We now consider the cladding. The goal is to realize the condition where k_{t2} is imaginary, in which case the propagating energy is confined. This can be realized if $\varepsilon_2 < \varepsilon_1$, where ε_2 is the dielectric function of the cladding. The associated dispersion equation is then

$$-k_{t2}^2 + k_z^2 = \frac{\omega^2 \varepsilon_2}{c^2}, \tag{14.51}$$

where k_{t2} is real. This is the second equation that must be satisfied. The equation for $\vec{E}_{z2}(\rho, t)$ in the cladding is therefore

$$E_{z2}(\rho, \varphi, z, t) = E_2 K_\nu(k_{t2}\rho) e^{i\nu\varphi} e^{ik_z z - i\omega t}, \tag{14.52}$$

where $K_\nu(z)$ is the modified Bessel function that converges exponentially for large argument.

Matching the axial and azimuthal tangential components of $\vec{E}_1(\vec{r}, t)$ and $\vec{E}_2(\vec{r}, t)$, and the azimuthal tangential components of $\vec{H}_1(\vec{r}, t)$ and $\vec{H}_2(\vec{r}, t)$ at $\rho = a$ leads to three conditions. The axial condition requires k_z to be the same in core and cladding, which is the third equation. The fourth equation follows from continuity of the electric fields across the $\rho = a$ boundary, considered along the *z* direction:

$$E_1 J_\nu(k_{t1}a) = E_2 K_\nu(k_{t2}a). \tag{14.53}$$

The continuity condition on the azimuthal component of $\vec{H}$ across the $\rho = a$ boundary establishes the fifth condition:

$$\left(1 + \frac{k_z^2}{k_{t1}^2}\right) J_\nu(k_{t1}a) = \left(1 + \frac{k_z^2}{k_{t2}^2}\right) K_\nu(k_{t2}a). \tag{14.54}$$

Taking to be obvious the fact that k_z must be the same across the boundary, the four remaining equations determine the values of the four remaining unknowns k_{t1}, k_z, k_{t2}, and the ratio of amplitudes across the boundary. This is clearly a computer problem, not something to be attempted on the back of an envelope.

The engineering challenge is to select frequencies, dielectric functions, and dimensions such that all these criteria are met. This obviously requires that $\varepsilon_1 > \varepsilon_2$, that is, the refractive index of the core must be larger than that of the cladding. In the single-mode configuration, energy remains in the fiber not because of multiple internal reflections, but because the solution outside the core decreases exponentially. In fact, a large fraction of the mode resides in the cladding. For this reason the cladding layer must be thick enough so the wave does not penetrate

appreciably to its outside. In that case the energy is confined. It cannot escape, and so is transmitted down the fiber.

H. Coaxial cables.

Coaxial cables have an inner and an outer conductor. This configuration can support a potential difference between the two equipotential surfaces. This makes it distinct from the waveguides discussed above, where the entire boundary is at a single potential. In particular, the possibility of a potential difference between the inner and outer conductors allows an electrostatic solution of the transverse Laplacian, for which the eigenvalue is zero. The dispersion equation then reduces simply to $k_z^2 = \omega^2/c^2$, so there is no cutoff. Hence coaxial cables can be used in dc applications, as everyone who has worked with a BNC cable knows.

The electric and magnetic fields for the electrostatic mode are both transverse to the propagation direction, so the mode is termed TEM. It is obtained quantitatively as follows. Let the cylindrical guide have a circular cross section of radius *b* contain a centrally located conductor also of circular cross section but of radius $a < b$. For mathematical simplicity we assume that the dielectric function of the insulating material separating the conductors is 1. The wave equation is

$$\left(\nabla_t^2 + \frac{\partial^2}{\partial z^2} - \frac{1}{c^2}\frac{\partial^2}{\partial t^2}\right)\vec{E}(\vec{r}_t)e^{ik_z z - i\omega t} = \left(\nabla_t^2 - k_z^2 + \frac{\omega^2}{c^2}\right)\vec{E}(\vec{r}_t)e^{ik_z z - i\omega t} = 0\,. \tag{14.55}$$

With an inner and an outer conductor the electric field can be radial, consistent with the electrostatic solution, and still satisfy boundary conditions on both conductors.

The standard approach is to write $\vec{E}(\vec{r}_t) = -\nabla\phi(\vec{r})$, where $\phi(\vec{r}) = \phi(\rho) = 4\pi\sigma\, a \ln(a/\rho)$ is the electrostatic potential set equal to zero at $\rho = a$. With no azimuthal dependence

$$\nabla_t^2\phi(\rho) = \frac{1}{\rho}\frac{\partial}{\partial\rho}\left(\rho\frac{\partial\phi}{\partial\rho}\right) + \frac{1}{\rho^2}\frac{\partial^2\phi}{\partial\varphi^2} = -\frac{4\pi\sigma a}{\rho}\frac{\partial}{\partial\rho}\left(\rho\frac{\rho}{a}\frac{a}{\rho^2}\right) = 0\,. \tag{14.56}$$

Interchanging the Laplacian and gradient operators, it follows that

$$\nabla_t^2\vec{E}(\vec{r}_t) = -\nabla_t^2\nabla\phi(\vec{r}) = -\nabla(\nabla_t^2\phi(\vec{r})) = 0\,.$$

While this is consistent with what we know about vector calculus, it is instructive to check the math anyway. The gradient operation in cylindrical coordinates is

$$\nabla_t = \hat{\rho}\frac{\partial}{\partial\rho} + \hat{\varphi}\frac{1}{\rho}\frac{\partial}{\partial\varphi}, \tag{14.57}$$

which yields

$$\vec{E}(\rho) = -\nabla\phi = 4\pi\sigma\, a\frac{\hat{\rho}}{\rho}\,. \tag{14.58}$$

With no obvious azimuthal dependence in the above, we evaluate the first term in the gradient, finding

$$\nabla_t^2 \vec{E}(\rho) = \frac{1}{\rho}\frac{\partial}{\partial\rho}\left(\rho\frac{\partial\phi}{\partial\rho}\right)4\pi\sigma a\frac{\hat{\rho}}{\rho} = \frac{4\pi\sigma a}{\rho^3}\hat{\rho}\,. \tag{14.59}$$

But this does not look like zero. Did we prove calculus wrong, or did we make a mistake? A second look at the Laplacian reveals that ∇_t^2 contains a second operator. The error is now clear: $\hat{\rho} = \hat{x}\cos\varphi + \hat{y}\sin\varphi$ is a function of φ. When the second term is taken into account, the result is the first term with a minus sign, so the final result is zero. Calculus is correct after all.

Because the field is an eigenfunction of the Laplacian with eigenvalue zero, the dispersion equation reduces to

$$\left(k_z^2 - \frac{\omega^2}{c^2}\right)\vec{E}(\vec{r}_t)e^{ik_z z - i\omega t} = 0\,, \tag{14.60}$$

so as noted above, k_z is real for all ω. There is no cutoff. The magnetic field can be obtained as usual according to

$$\vec{H} = -\frac{ic}{\omega}\nabla\times\vec{E} = -\frac{ic}{\omega}\hat{\varphi}\frac{\partial E_\rho}{\partial z} = \hat{\varphi}\frac{4\pi\sigma a}{\rho}. \tag{14.61}$$

Finally, the cycle-averaged power flow is

$$\vec{S} = \frac{c}{8\pi}\vec{E}\times\vec{H}^* = \frac{c}{8\pi}\left(\frac{4\pi\sigma a}{\rho}\right)^2\hat{z}\,. \tag{14.62}$$

To my knowledge, higher modes in a coaxial cable are never discussed, although it is a useful mathematical exercise to do so. For this calculation we assume that the potential of the inner and outer conductors is zero, and consider TM modes only. In this case $E_z = 0$ at $\rho = a$ and $\rho = b$. This is obviously impossible in general with the $J_\nu(k_{\nu n}\rho)$ alone, but with $\rho = 0$ excluded from consideration we can form a linear combination of $J_\nu(k_{\nu n}\rho)$ and $Y_\nu(k_{\nu n}\rho)$. Accordingly, let

$$E_{z,\nu n}(\rho,\varphi) = \left(A_{\nu n}J_\nu(k_{\nu n}\rho) + B_{\nu n}Y_\nu(k_{\nu n}\rho)\right)e^{i\nu\varphi}e^{ik_z z - i\omega t}, \tag{14.63a}$$

where

$$E_{z,\nu n}(a,\varphi) = E_{z,\nu n}(b,\varphi) = 0\,. \tag{14.63b}$$

Common values of $k_{\nu n}$, ν, and *n* are used throughout because the functions must match on both boundaries. The linear combination must therefore satisfy

$$A_{\nu n}J_\nu(k_{\nu n}a) + B_{\nu n}Y_\nu(k_{\nu n}a) = 0\,; \tag{14.64a}$$

$$A_{\nu n}J_\nu(k_{\nu n}b) + B_{\nu n}Y_\nu(k_{\nu n}b) = 0\,; \tag{14.64b}$$

or in matrix form

$$\begin{pmatrix} J_\nu(k_{\nu n}a) & Y_\nu(k_{\nu n}a) \\ J_\nu(k_{\nu n}b) & Y_\nu(k_{\nu n}b)\end{pmatrix}\begin{pmatrix} A_{\nu n} \\ B_{\nu n}\end{pmatrix} = 0\,. \tag{14.65}$$

We recognize this as a standard eigenvalue/eigenvector equation, with a nontrivial solution obtained by the setting the determinant of the (2×2) matrix equal to zero. The result defines a discrete infinity of values $k_{\nu n}$, which are then used to construct the modes.

To better appreciate that this procedure delivers eigenvalues, substitute $J_\nu(k_{\nu n}x)\to\cos(k_\nu x)$ and $Y_\nu(k_{\nu n}x)\to\sin(k_\nu x)$ in the above. Setting the determinant equal to zero in this case yields

$$\sin\left(k_{\nu n}(b-a)\right)=0\,. \tag{14.66}$$

It is evident that that this equation is satisfied only for certain values of $k_{\nu n}$.

I. Orthogonality in cross-sectional integrations; modes as basis functions.

Up to now we have focused on the longitudinal components $E_z(\vec{r}_t)$ and $H_z(\vec{r}_t)$ as the basic descriptors of modes. However, when considering the use of antennas to deliver energy to or from a mode, it is sometimes convenient to use cross sections $\vec{E}_t^{TM}=\nabla_t E_z(\vec{r}_t)$ and $\vec{H}_t^{TE}=\nabla_t H_z(\vec{r}_t)$. The reason is that maximally efficient transfer of power between an antenna and a guide requires the current distribution in the antenna to overlap exactly the cross-sectional spatial dependence of the intended mode. Otherwise energy is wasted by being delivered to unwanted modes. Profile-matching brings up questions of orthogonality in two-dimensional integrals over the cross section of the guide. Jackson lets the reader deal with the orthogonality issue in Probs. 8.18 and 8.19, and only cites incomplete results for antenna coupling in Sec. 8.12. However, because proof of orthogonality and the calculation involving coupling both contain some essential physics, it is worth giving each a separate section and going into these topics in detail.

Our objective in this section is to show that the transverse electric fields of TE and TM modes are universally orthogonal when integrated over the cross-section of the guide, and hence form a complete set that can be used as basis functions for expansions. While orthogonality applies to two-dimensional integrals, the divergence theorem on which it is based is three-dimensional. We adapt the divergence theorem to two dimensions by using a configuration that has no *z* dependence, hence the phase factor $e^{ik_z z-i\omega t}$ does not appear in the following. The derivations also take advantage of boundary conditions and the relations $\vec{E}_t=(ik_z/k_t^2)\nabla E_z$ and $\nabla_t^2 E_z=-k_t^2 E_z$. While the calculations are nontrivial, they can be considered to be a review of those leading in Ch. 2 to Green's Theorem, in addition to providing worthwhile examples of how applied math leads to useful results.

We consider the easier case first. The TM derivation starts with

$$\int_V d^3r'\,\nabla\cdot(E_{z,\mu}\nabla E_{z,\nu})=\int_S d^2r'\,\hat{n}\cdot(E_{z,\mu}\nabla E_{z,\nu})=0 \tag{14.67a}$$

$$=\int_V d^3r'\left(\nabla E_{z,\mu}\cdot\nabla E_{z,\nu}+E_{z,\mu}\nabla^2 E_{z,\nu}\right) \tag{14.67b}$$

$$=\Delta z\int_{X_{\text{sec}}} d^2r'\left(\nabla_t E_{z,\mu}\cdot\nabla_t E_{z,\nu}+E_{z,\mu}k_{t,\nu}^2 E_{z,\nu}\right) \tag{14.67c}$$

Here, $E_{z,\mu} = E_{z,\mu}(\vec{r}_t)$ and $E_{z,\nu} = E_{z,\nu}(\vec{r}_t)$ are the *z* components of the μ and *v* modes, respectively, X_{sec} is the cross-section of the guide perpendicular to the *z* axis, and *V* is the volume enclosed between two cross sections that are separated by a distance Δz (see diagram). Because there is no *z* dependence the *z*-integration is trivial. The surface integral vanishes because $E_{z,\mu}$ is zero on the periphery and – even if the end-cap integrals were nonzero - the normal vectors on the end caps point in opposite directions. What remains are the cross-section integrals that we want.

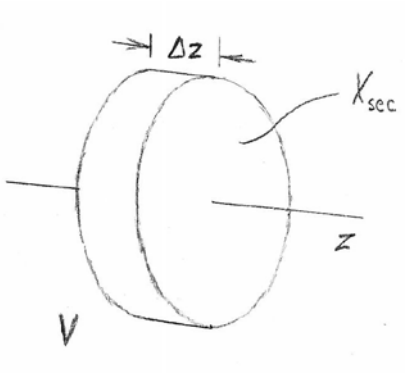

We now repeat the derivation with the components $E_{z,\mu}$ and $E_{z,\nu}$ interchanged, and subtract the result from the former expression (recall the derivation of Green's Theorem in Ch. 2.) The scalar product of the two gradients vanishes in subtraction, leaving

$$(k_{t,\mu}^2 - k_{t,\nu}^2) \int_{X_{\text{sec}}} d^2r' E_{z,\mu} E_{z,\nu} = 0 . \tag{14.68}$$

Thus either the eigenvalues of modes μ and *v* are the same, in which case the levels are degenerate, or the *z* components of different modes are orthogonal.

However, we are interested in the orthogonality of the *transverse*, not longitudinal, fields. To accomplish this, return to the starting point, writing for $\mu \neq \nu$:

$$\int_V d^3r' \left(\nabla E_{z,\mu} \cdot \nabla E_{z,\nu} + E_{z,\mu} \nabla^2 E_{z,\nu} \right) = \Delta z \int_{X_{\text{sec}}} d^2r' \left(\nabla_t E_{z,\mu} \cdot \nabla_t E_{z,\nu} + k_{t,\nu}^2 E_{z,\mu} E_{z,\nu} \right) \tag{1469a}$$

$$= \Delta z \int_{X_{\text{sec}}} d^2r' (\nabla_t E_{z,\mu} \cdot \nabla_t E_{z,\nu}) \tag{14.69b}$$

$$= -\frac{k_{t,\mu}^2 k_{t,\nu}^2}{k_z^2} \Delta z \int_{X_{\text{sec}}} d^2r' \vec{E}_{t,\mu} \cdot \vec{E}_{t,\nu} = 0 . \tag{14.69c}$$

In Eq. (14.69b) we have taken advantage of Eq. (14.68). Thus the scalar product of the transverse TM electric fields is indeed orthogonal when integrated over the cross section of the guide.

The derivation for the TE calculation proceeds identically starting with the *z* components of the magnetic fields. Here, circumference part of the surface integral vanishes because $\frac{\partial H_{z,\mu}}{\partial n}$ is zero on the perimeter of the guide. Once the orthogonality relation

$$(k_{t,\mu}^2 - k_{t,\nu}^2) \int_{X_{\text{sec}}} d^2r' H_{z,\mu} H_{z,\nu} = 0 \tag{14.70}$$

is established, the parallel calculation yields

$$\int_V d^3r' \left(\nabla H_{z,\mu} \cdot \nabla H_{z,\nu} + H_{z,\mu} \nabla^2 H_{z,\nu} \right) = -\frac{k_{t,\mu}^2 k_{t,\nu}^2}{k_z^2} \int_{X_{\text{sec}}} d^2r' \vec{H}_{t,\mu} \cdot \vec{H}_{t,\nu} = 0 , \tag{14.71}$$

for $\mu \neq \nu$. Now, using

$$\vec{E} = -\frac{k}{k_z}\hat{z}\times\vec{H}\ , \tag{14.72}$$

we work backward as

$$\int_{X_{\text{sec}}} d^2r\,\vec{E}_{t,\mu}\cdot\vec{E}_{t,\nu} = \frac{k^2}{k_z^2}\int_{X_{\text{sec}}} d^2r\,(\hat{z}\times\vec{H}_{t,\mu})\cdot(\hat{z}\times\vec{H}_{t,\mu}) = \frac{k^2}{k_z^2}\int_{X_{\text{sec}}} d^2r\,\hat{z}\cdot\vec{H}_{t,\mu}\times(\hat{z}\times\vec{H}_{t,\mu}) \tag{14.73a}$$

$$= \frac{k^2}{k_z^2}\int_{X_{\text{sec}}} d^2r\,\hat{z}\cdot\vec{H}_{t,\mu}\times(\hat{z}\times\vec{H}_{t,\mu}) \tag{14.73b}$$

$$= \frac{k^2}{k_z^2}\int_{X_{\text{sec}}} d^2r\,\hat{z}\cdot\left((\vec{H}_{t,\mu}\cdot\vec{H}_{t,\nu})\hat{z} - (\vec{H}_{t,\mu}\cdot\hat{z})\vec{H}_{t,\nu}\right) \tag{14.73c}$$

$$= \frac{k^2}{k_z^2}\int_{X_{\text{sec}}} d^2r\,\vec{H}_{t,\mu}\cdot\vec{H}_{t,\nu} = 0 \tag{14.73d}$$

if $\mu \neq \nu$. Thus we can use electric fields as basis functions for both TE and TM modes.

The mixed mode remains to be considered. This is an interesting challenge because the surface integral does not vanish when considering the combination $\nabla\cdot(H_{z,\mu}\nabla E_{z,\nu})$. In fact for a rectangular guide it is easy to show that the cross-sectional integral of $H_{z,\mu}E_{z,\nu}$ cannot vanish in general. Let

$$E_{z,mn}(\vec{r}_t) = E_{mn}\sin\left(\frac{\pi m}{a}x\right)\sin\left(\frac{\pi n}{b}y\right), \tag{14.74a}$$

$$H_{z,m'n'}(\vec{r}_t) = H_{m'n'}\cos\left(\frac{\pi m'}{a}x\right)\cos\left(\frac{\pi n'}{b}y\right). \tag{14.74b}$$

Then

$$\int_0^a dx\int_0^b dy E_{mn}H_{m'n'}\sin\left(\frac{\pi m}{a}x\right)\sin\left(\frac{\pi n}{b}y\right)\cos\left(\frac{\pi m'}{a}x\right)\sin\left(\frac{\pi n'}{b}y\right). \tag{14.75}$$

This is the product of two integrals of the form

$$\int_0^a dx\sin\left(\frac{\pi m}{a}x\right)\cos\left(\frac{\pi m'}{a}x\right) = -\frac{a}{2\pi}\int_0^\pi d\theta\left(\sin((m+m')\theta)+\sin((m-m')\theta)\right) \tag{14.76a}$$

$$= 0 \text{ if } (m+m') \text{ is even;} \tag{14.76b}$$

$$= \frac{2am}{\pi(m^2-m'^2)} \text{ if } (m+m') \text{ is odd.} \tag{14.76c}$$

Thus in the mixed-mode case, no general orthogonality relation on the *z* components exists.

Nevertheless, the corresponding transverse fields of mixed modes are orthogonal in general. To show this consider

$$\int_V d^3r \vec{E}_{t,\mu}^{TM} \cdot \vec{E}_{t,\nu}^{TE} = \Delta z \int_{X_{\text{sec}}} d^2r \vec{E}_{t,\mu}^{TM} \cdot \vec{E}_{t,\nu}^{TE} \tag{14.77a}$$

$$= \frac{ik_z}{k_{t,\mu}^2} \int_V d^3r \nabla E_{z,\mu}^{TM} \cdot (\hat{z} \times \vec{H}_{t,\nu}^{TE}) \tag{14.77b}$$

$$= \frac{ik_z}{k_{t,\mu}^2} \int_V d^3r \left(\nabla \cdot \left(E_{z,\mu}^{TM} (\hat{z} \times \vec{H}_{t,\nu}^{TE}) \right) - E_{z,\mu}^{TM} \nabla \cdot (\hat{z} \times \vec{H}_{t,\nu}^{TE}) \right). \tag{14.77c}$$

When converted to a surface integral the divergence term vanishes because $E_{z,\mu}^{TM}$ is zero on the outer surface of the guide, and the normal vectors on the side point in opposite directions. The divergence of the second term can be expanded as

$$\nabla \cdot (\hat{z} \times \vec{H}_{t,\nu}^{TE}) = \vec{H}_{t,\nu}^{TE} \cdot (\nabla \times \hat{z}) - \hat{z} \cdot (\nabla \times H_{t,\nu}^{TE}). \tag{14.78}$$

The first term vanishes because $\hat{z}$ is a constant. The second term vanishes because $H_{t,\nu}^{TE}$ is the gradient of $H_{z,\nu}$, and the curl of a gradient vanishes. Although the argument can be raised that $\vec{H}_{t,\nu}^{TE}$ is the result of only the *transverse* gradient acting on H_z^{TE}, the fact that everything is independent of *z* means that the *z* part of the gradient is zero. Thus in general

$$\int_{X_{\text{sec}}} d^3r \, \vec{E}_{t,\mu}^{TM} \cdot \vec{E}_{t,\nu}^{TE} = 0 \tag{14.79}$$

for *all* μ and ν, including $\mu = \nu$.

This completes the proof that $\vec{E}_{t,\mu}^{TM}$ and $\vec{E}_{t,\nu}^{TE}$ form a complete set of orthogonal functions. Any cross-sectional function in the waveguide can therefore be expanded in terms of them.

As a side application, we consider power transmitted down a waveguide by a collection of TM waves. Writing the collection as

$$\vec{E}(\vec{r},t) = \sum_\mu (\vec{E}_{t,\mu} + \hat{z} E_{z,\mu}) \tag{14.80}$$

and using

$$\vec{H}(\vec{r},t) = \sum_\nu \frac{k}{k_{z,\nu}} \hat{z} \times \vec{E}_{t,\nu}, \tag{14.81}$$

it follows that

$$I_{tot} = \frac{c}{4\pi} \int_{X_{\text{sec}}} d^2r \, \hat{z} \cdot \vec{E} \times \vec{H} = \frac{c}{4\pi} \int_{X_{\text{sec}}} d^2r \sum_{\mu,\nu} \frac{k}{k_{z,\nu}} \hat{z} \cdot \left((\vec{E}_{t,\mu} + \hat{z} E_{z,\mu}) \times (\hat{z} \times \vec{E}_{t,\nu}) \right) \tag{14.82a}$$

$$= \frac{c}{4\pi} \sum_{\mu,\nu} \frac{k}{k_{z,\mu}} \int_{X_{\text{sec}}} d^2r \, \hat{z} \cdot \left((\vec{E}_{t,\mu} \cdot \vec{E}_{t,\nu}) \hat{z} - E_{z,\mu} \vec{E}_{t,\nu} \right) \tag{14.82b}$$

$$= \frac{c}{4\pi} \sum_{\nu} \frac{k}{k_{z,\nu}} \int_{X_{\text{sec}}} d^2 r \, \vec{E}_{t,\nu}^{\,2} \, . \tag{14.82c}$$

Thus the total intensity is the sum of the individual intensities, which is what we expect.

The same result is obtained for TE modes, but if written in terms of $\vec{E}_t$, the prefactor k/k_z is inverted. This completes the discussion of orthogonality.

J. Energy transfer: mode/antenna coupling in waveguides.

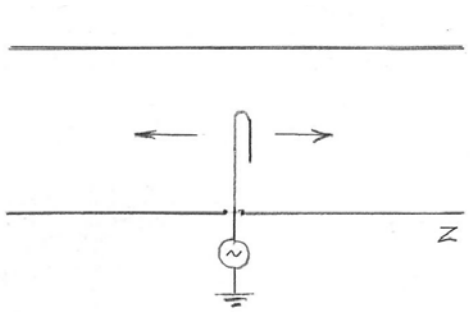

We now consider how these modes originate via their interactions with an antenna in the waveguide. This can be considered a precursor to Ch. 15 on radiation. Jackson gives a brief discussion in his Sec. 8.12, but by leaving time out of the picture, confusion is created in addition to missing basic physics. The topic provides an excellent example of why one should avoid the $\vec{E} \times \vec{H}^*$ approach when working with power and energy. The interesting questions concern not only the missed physics, but why it was missed and what can be done to avoid similar difficulties in the future.

The problem that we are addressing is illustrated in the diagram. The waveguide contains an antenna located at $z = 0$. The antenna is described by its current flow

$$\vec{J}(\vec{r},t) = \vec{K}(\vec{r}_t)\delta(z)e^{-i\omega t} \tag{14.83}$$

where $\vec{K}(\vec{r}_t)$ is a surface current. We assume that the guide also contains a rightward-propagating mode with an electric field

$$\vec{E}(\vec{r},t) = (\hat{x}E_x + \hat{y}E_y + \hat{z}E_z)e^{ik_z z - i\omega t + i\varphi} \, , \tag{14.84}$$

where E_x, E_y, and E_z are functions of $\vec{r}_t$ and φ is a phase factor that allows for the possibility that the phases of $\vec{J}$ and $\vec{E}$ may be different at $z = 0$. For a TE wave $E_z = 0$.

In Ch. 1 we derived the general energy expression

$$\vec{J} \cdot \vec{E} = -\nabla \cdot \left(\frac{c}{4\pi} \vec{E} \times \vec{H} \right) - \frac{1}{4\pi} \vec{H} \cdot \frac{\partial \vec{B}}{\partial t} - \frac{1}{4p} \vec{E} \cdot \frac{\partial \vec{D}}{\partial t} , \tag{14.85}$$

which has obvious possibilities: an integration over two planes $z = \pm \delta z$ where $\delta z \to 0$ will capture the energy transfer between the mode and the antenna, while Gauss' Theorem allows the divergence term to be converted to two surface integrals that describe the energy entering and/or leaving the region. We recall that the quantities entering the nonlinear Eq. (14.85) must be real. Considering first the time derivatives, with a hollow guide $\vec{D} = \vec{E}$ so the volume term in the electric-field case follows from

$$\text{Re}\left(\vec{E}(\vec{r},t) \right) = \vec{E}(\vec{r}_t)\cos(kz - \omega t + \varphi) \, ; \tag{14.86a}$$

$$\mathrm{Re}\left(\frac{\partial \vec{E}(\vec{r},t)}{\partial t}\right) = \omega \vec{E}(\vec{r}_i)\sin(kz-\omega t+\varphi)\,. \tag{14.86b}$$

The time average of the product of these two terms is zero. Thus energy does not accumulate locally, as expected. The same result applies to the time average of the volume term in the magnetic-field case.

To evaluate the Poynting vector, write

$$\vec{H}(\vec{r},t) = -\frac{ic}{\omega}\nabla\times\vec{E}$$

$$= \frac{-ic}{\omega}\begin{vmatrix} \hat{x} & \hat{y} & \hat{z} \\ \dfrac{\partial}{\partial x} & \dfrac{\partial}{\partial y} & \dfrac{\partial}{\partial z} \\ E_x e^{ik_z z} & E_y e^{ik_z z} & E_z e^{ik_z a} \end{vmatrix} e^{-i\omega} \tag{14.87}$$

Carrying through the math

$$\vec{H}(\vec{r},t) = -\frac{ic}{\omega}\left(\hat{x}\left(\frac{\partial E_z}{\partial y} - ik_z E_y\right) - \hat{y}\left(\frac{\partial E_z}{\partial x} - ik_z E_x\right) + \hat{z}\left(\frac{\partial E_y}{\partial x} - \frac{\partial E_x}{\partial y}\right)\right)e^{ik_z z - i\omega t + i\varphi}\,; \tag{14.88a}$$

$$\mathrm{Re}\left(\vec{H}(\vec{r},t)\right) = \frac{c}{\omega}\left(\hat{x}\frac{\partial E_z}{\partial y} - \hat{y}\frac{\partial E_z}{\partial x} + \hat{z}\left(\frac{\partial E_y}{\partial x} - \frac{\partial E_x}{\partial y}\right)\right)\sin(k_z z-\omega t+\varphi)$$

$$+\frac{ck_z}{\omega}\left(-\hat{x}E_y + \hat{y}E_x\right)\cos(k_z z-\omega t+\varphi)\,. \tag{14.88b}$$

In the cross product the time average of the first term vanishes, leaving the second term. Performing the necessary operations we obtain

$$\vec{S} = \frac{c}{4\pi}\hat{z}\left(E_x^2 + E_y^2\right)\cos^2(k_z z-\omega t+\varphi)\,. \tag{14.89}$$

We now consider the volume integral over a small region containing the antenna using Eqs. (14.83) and (14.85). The result is

$$\int_V d^3r'\,\vec{K}\cdot\vec{E} = \int_S d^2r'\left(K_x E_x + K_y E_y\right)\cos(\omega t)\cos(\omega t-\varphi)$$

$$= \left(\int_S d^2r'\left(K_x E_x + K_y E_y\right)\right)\left(\cos^2\omega t\cos\delta - \cos\omega t\sin\omega t\sin\delta\right). \tag{14.90}$$

The surface integrals over the $\pm\delta z$ planes bounding the antenna reduce to

$$\int_V d^3r'\,\nabla\cdot S = \int_S d^2r'\left(\left(E_x^2+E_y^2\right)_+ - \left(E_x^2+E_y^2\right)_-\right)\cos^2\omega t\,. \tag{14.91}$$

Performing the time averages leads to

$$\frac{1}{2}\int_S d^2r'\left(\left(E_x^2+E_y^2\right)_+ -\left(E_x^2+E_y^2\right)_-\right)=\frac{c}{8\pi}\int_S d^2r'\left(K_xE_x+K_yE_y\right)\cos\varphi\,. \tag{14.92}$$

Equation (14.92) shows that the antenna can either deliver power to or extract power from the wave depending on whether the power factor $\cos\varphi$ is positive or negative. Using the results of the previous section, optimal delivery to a single mode (and nondelivery to orthogonal modes) occurs if the spatial dependence of the surface current $\vec{K}$ matches the cross-sectional variation of the desired mode. The sign of the left side of the equation can be interpreted as a direction if inconsistent with the positive-definite nature of the integrand. Thus if there were no incoming wave, Eq. (14.92) would be interpreted as power being delivered equally to modes propagating in the positive and negative *z* directions. Thus a consistent picture is obtained.